ELSEVIER

Polymer 40 (1999) 6811–6820

polymer

Monitoring phase separation and reaction advancement in situ in thermoplastic/epoxy blends

S. Poncet[a], G. Boiteux[a], J.P. Pascault[a], H. Sautereau[a], G. Seytre[a], J. Rogozinski[b], D. Kranbuehl[b,*]

[a]*INSA and UCB, UMR-CNRS 5627, 69621 Villeurbanne, France*
[b]*Departments of Chemistry and Applied Science, College of William and Mary, Williamsburg, VA 23187, USA*

Received 16 October 1998; accepted 29 January 1999

Abstract

Frequency-dependent dielectric measurements have been used to monitor and characterize the phase separation process in high-performance thermoplastic–thermoset blends of 2,6-dimethyl-1,4-phenylene ether (PPE) with an epoxy diglycidylether of bisphenol A (DGEBA) and 4,4-methylene bis(3-chloro-2,6-diethylamine) (MCDEA). The systems studied are 30, 45 and 60% PPE/DGEBA–MCDEA blends. The results are compared with dynamical mechanical measurements and the developing morphology.

Both dielectric and mechanical measurements are shown to be good techniques to monitor the phase-separation process and the reaction advancement. Dielectric measurements monitor the buildup in T_g in both the PPE-rich continuous phase and in the epoxy-rich occluded phases. Dielectric measurements are advantageous as they can be made in situ continuously on a single sample throughout the entire cure process. The results show that the phase separation process initially occurs rapidly involving a large amount of the epoxy–amine diffusing into the occluded phase. The rate of the epoxy–amine reaction in the epoxy-rich 30% PPE mixture is approximately equal to that in the neat epoxy–amine system due to two opposing effects, a slower reaction rate due to dilution and a lower level of conversion at vitrification due to the presence of high T_g PPE. In the 60% PPE mixture, the dilution effect of the PPE has a large affect on the decreasing the reaction rate and achievement of vitrification. The continuous thermoplastic-rich phase is observed to vitrify first, followed by vitrification of the thermoset as occluded particles. Finally, the results show as evidenced by the size of the occluded particles and the composition of the continuous phase that the morphology is strongly influenced by the kinetics, diffusion, and viscosity conditions during phase separation.

Keywords: Thermoplastic/epoxy blends; Phase separation; Dielectric

1. Introduction

The development of high-temperature, high-performance thermoplastic polymeric materials presents several major challenges. Besides possessing a high glass transition temperature, the polymer must have the toughness of a thermoplastic and the strength of a thermoset. In addition, the polymeric material should have a processable viscosity at an acceptable temperature. One of the most promising approaches for achieving these often opposing material properties is through thermoplastic–thermoset blends. The use of thermoset–thermoplastic blends has been widely studied as a means to toughen the polymer network, to improve the surface finish of molded parts, to reduce thermal stress and to introduce structure such as micropores [1–5].

With the recent development of high-temperature, high-performance thermoplastics, examples being polyetherimide (PEI), poly(2,6-dimethyl-1,4-phenylene ether or oxide) (PPE or PPO) and poly(ether ether ketone) (PEEK), the blending of thermosets with these high glass transition thermoplastics is a potentially novel way to improve their processability [6–13]. Often because of their high glass transition temperature and high viscosity, these thermoplastics are too difficult to mold or suffer degradation at temperatures where viscosity makes processing possible. The addition of an appropriate reactive solvent, the thermoset precursor, significantly reduces the softening temperature. This unique approach has been termed “reactive processing” [1,6,7].

The advantage of blending the thermoset precursor with the thermoplastic is that the softening temperature is decreased significantly. But this advantage creates additional complexity and the potential for variability during processing. First, the processing time is now controlled by

* Corresponding author. Tel. + 1-757-221-2540; fax: + 1-757-221-2715.
E-mail address: dekran@chem1.chem.wm.edu (D. Kranbuehl)

0032-3861/99/$ - see front matter
PII: S0032-3861(99)00104-4

the thermoset precursor reactivity. As it reacts increasing its molecular weight, the entropy of mixing decreases. The entropy term ΔS^m usually dominants the free energy of mixing $\Delta G^m = \Delta H^m - T\Delta S^m$. Thus as the molecular weight increases, an average molecular weight is reached where a homogeneous mixture is no longer favored, and the thermoplastic-reacting thermoset system separates into two phases. One phase is called the α-phase, which is rich in thermoset. The other is called the β-phase and is rich in thermoplastic. For most thermoplastic–epoxy resin ratios with 25% or more by weight thermoplastic, the new phase separated system is a continuous β-phase with occluded α-phase spheres. At this point as a result of both phase separation and advancement of the epoxy–amine reaction, the viscosity increases rapidly. It has been shown that the viscosity at the cloud point and the conditions of phase separation can have a strong effect on the final morphology and mechanical properties [13].

As a consequence, while making processing of high-temperature thermoplastics possible at significantly lower temperatures, there are new concerns and quantities that need to be monitored. One quantity of concern is the time of the onset of phase separation. This is the point at which the viscosity starts to rise. Second, the advancement of the reacting thermoset precursor needs to be monitored. The time–temperature history of both the onset of phase separation and reaction advancement are important in knowing and controlling the morphology. Finally, achievement of an acceptable T_g and full cure needs to be known for both phases.

This paper discusses the use of dynamic mechanical and frequency-dependent dielectric measurements to monitor the time of phase separation and the reaction advancement as monitored by the buildup in T_g. The dielectric sensor measurements discussed in this report have the additional advantage that they can be made both in the laboratory as well as in situ in the fabrication tool in the production environment. The systems studied are 30, 45 and 60% by weight PPE/epoxy-hardener blends. A reactive precursor solvent of epoxy and hardener was chosen which reacts slowly and which has been well characterized [14,15]. The dielectric measurements are sensitive to interfacial charge polarization and have the ability to detect the onset of phase separation. The onset of phase separation is also detected by mechanical measurements through the increase in viscosity. Dielectric dipolar relaxation peaks at longer times monitor vitrification through the α-relaxation process in both phases. The mechanical relaxation measurements of the loss modulus peak also monitor the vitrification processes.

2. Experimental

Mixtures of 30, 45 and 60% PPE distributed by General Electric as PPE800 and PPE820 with $\bar{M}_n = 12\,000$, $\bar{M}_w = 25\,000$ g/mol were blended with an epoxy diglycidyl-ether of bisphenol A (DGEBA) from DOW, DER 332, 345.5 g/mol and a stoichiometric amount of 4,4-methylene bis(3-chloro-2,6-diethylaniline) (MCDEA) 380 g/mol, sold by LONZA.

The DGEBA and the MCDEA were mixed at 80°C using an IKA dual blade mixer. The epoxy–amine mixture was introduced into a twin screw corotative extruder from Clextral and extruded at 175°C. After extrusion it was determined the PPE–DGEBA–amine blend advancement was between 0.03 and 0.07.

Dynamic mechanical measurements were made using a Rheometrics RDA II in both laboratories using 25 mm plates, 1.5 mm gap, strain $< 3\%$ at 10 rad/s in a temperature-controlled chamber.

Frequency-dependent complex dielectric measurements were made using an impedance analyzer controlled by a microcomputer. In the work discussed here, measurements at frequencies from Hz to MHz are taken continuously throughout the entire cure process at regular intervals and converted to the complex permittivity, $\epsilon^* = \epsilon' - i\epsilon''$. The measurements are made with a geometry-independent interdigitated electrode [16]. The sensor is inserted into the blend and the impedance is measured with either a Hewlett Packard or a Schlumberger impedance bridge. This system permits multiplexed measurement of sensors. The sensor itself is planar, 1 × 1/2 inch in area and 5 mm thick. This sensor–bridge microcomputer assembly is able to make continuous uninterrupted measurements of both ϵ' and $\epsilon''$and over 10 decades in magnitude at all frequencies. The sensor is inert and has been used at temperatures exceeding 400°C and a pressure over 1000 psi [16].

3. Background

Frequency-dependent measurements of the dielectric impedance of a material as characterized by its equivalent capacitance (C) and conductance (G) are used to calculate the complex permittivity, $\epsilon^* = \epsilon' - i\epsilon''$, where $\omega = 2\pi f$, f is the measurement frequency and C_0 is the equivalent air replacement capacitance of the sensor.

$$\epsilon'(\omega) = \frac{C(\omega)\ \text{material}}{C_0} \tag{1}$$

$$\epsilon''(\omega) = \frac{G(\omega)\ \text{material}}{\omega C_0}.$$

This calculation is possible when using the sensor whose geometry is invariant over all measurement conditions. Both the real and the imaginary parts of ϵ^* can have dipolar (d) and ionic (i)-charge components.

$$\epsilon' = \epsilon'_d + \epsilon'_i \tag{2}$$

$$\epsilon'' = \epsilon''_d + \epsilon''_i.$$

Plots of the product of frequency (ω) multiplied by the

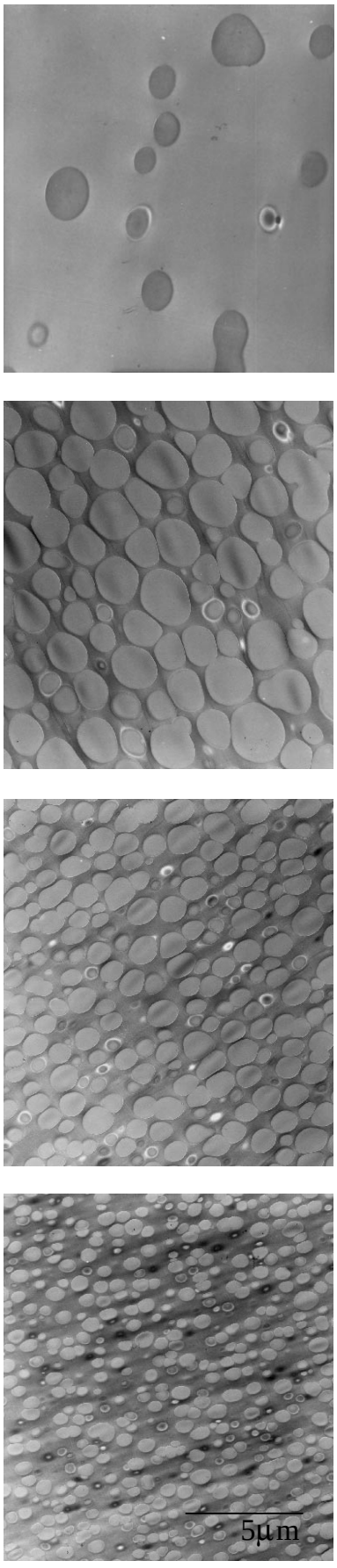

Fig. 1. TEM photos of the final morphology after 175°C isothermal cure and a post-cure at 200°C for a 10% (top), 30%, 45% and 60% PPE/DGEBA–MCDEA mixture.

imaginary component of the complex permittivity $\epsilon''(\omega)$ make it relatively easy to visually determine when the low frequency magnitude of ϵ'' is dominated by the mobility of ions and when at higher frequencies the rotational mobility of bound charge dominates ϵ''. Generally, the magnitude of the low-frequency overlapping values of $\omega\epsilon''(\omega)$ can be used to measure the change with time of the ionic mobility through the parameter σ where

$$\sigma(\text{ohm}^{-1}\ \text{cm}^{-1}) = \epsilon_0 \omega \epsilon_i''(\omega) \tag{3}$$

$$\epsilon_0 = 8.854 \times 10^{-14}\ \text{C}^2\ \text{J}^{-1}\ \text{cm}^{-1}.$$

The changing value of the ionic mobility is a molecular probe which can be used to monitor changes in the viscosity during cure. The dipolar component of the loss at higher frequencies can then be determined by subtracting the ionic component.

$$\epsilon''(\omega)\text{dipolar} = \epsilon''(\omega) - \frac{\sigma}{\omega\epsilon_0}. \tag{4}$$

The peaks in ϵ'' dipolar (which are usually close to the peaks in ϵ'') can be used to determine the time or point in the cure process when the "mean" dipolar relaxation time has attained a specific value $\tau = 1/\omega$, where $\omega = 2\pi f$ and f is the frequency of measurement. The dipolar mobility as measured by the mean relaxation time τ is monitoring the α-relaxation process associated with vitrification and it can be used as a molecular probe of the buildup in T_g. For example, the time of occurrence of a given dipolar α-relaxation time as measured by a peak in a particular high frequency value of $\epsilon''(\omega)$ can be quantitatively related to the attainment of a specific value of the glass transition temperature [16–23].

Interfacial polarization processes which occur in heterogeneous dielectrics will be present at the onset of phase separation, that is beginning at the onset of the transition from a homogeneous to a heterogeneous two-phase system [24–33]. These effects arise at the interface of two media having differing permittivities and conductivities. These interfacial effects can be quite strong sometimes creating increases in ϵ' by factors of 10 and a charge polarization relaxation time. The effect is dependent on the magnitude of the conductivity difference $(\sigma_2 - \sigma_1)$ between the occluded phase σ_2, and the continuous phase, σ_1.

The most well-known theoretical model of this effect is the Maxwell–Wagner–Sillars model [34–36]. Using the Maxwell–Wagner–Sillars model, the complex dielectric permittivity of the mixture $\epsilon^*(\omega)$ of orientated occluded ellipsoids with complex dielectric constant, $\epsilon_2^*(\omega)$, at a volume fraction v_2 dispersed in a continuous matrix with a complex dielectric constant, $\epsilon^*_1(\omega)$, can be calculated from

the following equation:

$$\epsilon^* = \epsilon^*_1 \frac{\epsilon^*_1(1-\nu_2)(1-A) + \epsilon^*_2(\nu_2 + A(1-\nu_2))}{\epsilon^*_1 + A(1-\nu_2)(\epsilon^*_2 - \epsilon^*_1)} \quad (5)$$

where $A(0 \leq A \leq 1)$, is the depolarization factor of the ellipsoidal filler particles. It depends on the shape of the particles (length of the long a to b short axis ratio for spheroids) and of the orientation of the field relative to the particle. For prolates spheroids (rod or needle-like) oriented along the shorter axis, A lies between 0 and 1/3, while for oblates spheroids (disc-like) oriented on the shorter axis, A lies between 1/3 and 1. For spheres $A = 1/3$.

Separating the real and imaginary parts leads to Debye's equations

$$\epsilon' = \epsilon_\infty + \frac{\epsilon_s - \epsilon_\infty}{1 + (\omega\tau)^2} \quad (6)$$

$$\epsilon'' = (\epsilon_s - \epsilon_\infty)\frac{\omega\tau}{1 + (\omega\tau)^2} \quad (7)$$

where $\omega = 2\pi f$ with explicit formulae for the low-and high-frequency limiting permittivity ϵ_s, ϵ_∞, and τ_{MWS} the relaxation time of the interfacial charge polarization.

$$\tau_{TMS} = \epsilon_0 \frac{\epsilon_2 + A(1-\nu_2)(\epsilon_2 - \epsilon_1)}{\sigma_1 + A(1-\nu_2)(\sigma_2 - \sigma_1)} \quad (8)$$

$$\epsilon_s = \epsilon_1 \frac{\sigma_1 + [A(1-\nu_2) + \nu_2](\sigma_2 - \sigma_1)}{\sigma_2 + A(1-\nu_2)(\sigma_2 - \sigma_1)} + \nu_2\sigma_1 \times \frac{[\sigma_1 + A(\sigma_2 - \sigma_1)](\epsilon_2 - \epsilon_1) - [\epsilon_1 + A(\epsilon_2 - \epsilon_1)](\sigma_2 - \sigma_1)}{[\sigma_1 + A(1-\nu_2)(\sigma_2 - \sigma_1)]^2} \quad (9)$$

where ϵ_0 denotes permittivity of free space, σ_1 and σ_2 are the conductivities of each phase, ϵ_1 and ϵ_2 are the limiting low-frequency permittivities for which by definition $\epsilon'' = 0$. An extended MWS model for randomly orientated ellipsoids shows that in such a case a distribution in the morphology (shape and/or orientation) of the occluded ellipsoids leads to a distribution of the relaxation times because of the distribution of the A values.

4. Results and discussion

The three mixtures of 30, 45 and 60% by weight PPE were cured at four temperatures 150, 175, 200 and 225°C. The TEM analysis photos in Fig. 1 display of the final morphology after curing isothermally at 175°C for 5 h followed by a 2-h post-cure at 200°C to fully cure the epoxy. For 30, 45 and 60% by weight PPE, the photos show phase separation with α-phase occluded particles in a continuous β-phase as opposed to the reverse in a 10% by weight PPE mixture. The photos also show a variation in particle size as the weight% of PPE increases. These results are reported in Table 1.

As a representative plot of the mechanical measurement results, Figs. 2 and 3 show the results at 175°C at 10 rad/s, strain $< 3\%$, using 25 mm plate, 1.5 mm gap for the 45% PPE blend. The values of G', G'', δ and η^* all show distinct changes with time. First at 35 min, there is a sharp rise of G' or η^* which is attributed to the onset of phase separation. It is known for PPE–epoxy blends that in mixtures of 25% or greater PPE, phase separation–inversion occurs where the continuous β-phase is rich in PPE [6–8]. This results in the continuous β-phase becoming richer in PPE, less plasticized and the viscosity rises rapidly. The important practical consequence of this effect is that by blending a reactive epoxy with PPE the initial processing temperature for flow of this otherwise high-viscosity, high-performance thermoplastic is significantly reduced even below its T_g of 213°C. The onset of a PPE-rich phase vitrification peak for 10 rad/s is observed in δ (and G'') curve at 70 min and peak at 86 min. The elapsed times in minutes to the mechanically observed onset of phase separation are reported in Table 2 for the three mixtures and the four isothermal reaction temperatures.

Mechanical measurements are difficult to make in a processing tool environment. Furthermore they reflect macroscopic force–displacement changes. Thus it is of interest to examine the ability of dielectric, electric field molecular force–displacement measurements of ions and dipoles to detect the phase separation and advancement of cure in this reactive epoxy/thermoplastic system.

Figs. 4 and 5 display the dielectric in situ sensor measurements of $\log[\omega\epsilon''(\omega)]$ and ϵ'. Both ϵ'' and ϵ' and show a sharp rise due to an interfacial charge polarization at 36 min. This large increase in η' and ϵ'' is due to the onset of phase separation of occluded regions rich in a more conductive epoxy–amine surrounded by the much less conductive PPE-rich continuous phase. Table 2 reports the elapsed time of the dielectric observed onset of phase separation.

The dielectric measurement detects the onset of phase separation as a charge polarization which arises with the onset of phase separation over molecular dimensions. The dielectric sensitivity to change in capacitance can be

Table 1
Morphologies of various PPE/DGEBA–MCDEA blends

Wt.% PPE	Initial volume % PPE	Final volume % continuous phase	Average diameter of occluded particles (μm)
30%	27.3	28 ± 2	2.3 ± 2.7
45%	40.5	43 ± 2	1.3 ± 0.09
60%	58	64 ± 2	0.76 ± 0.3

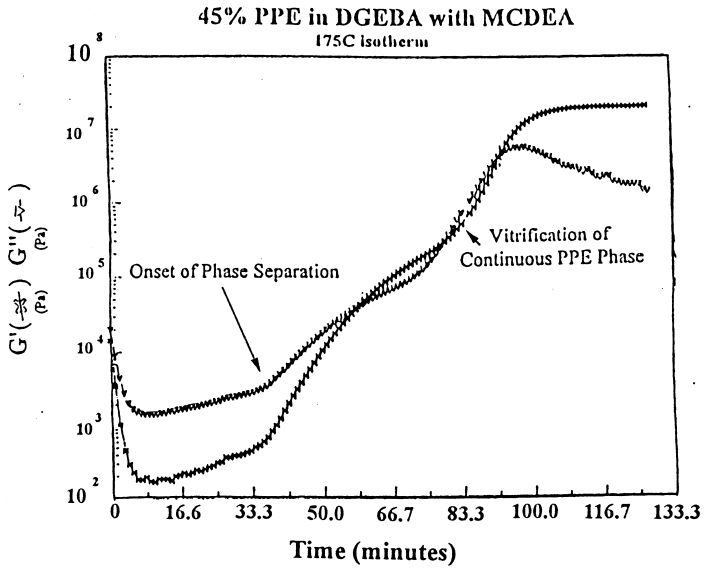

Fig. 2. Dynamic mechanical values of modulus G' and G'' versus time for the 45% PPE/DGEBA–MCDEA cured at 175°C.

thought of as a charge/distance ratio, which can be large even for small values in charge polarization if the molecular distance is small. On the other hand, changes in mechanical properties are generally observed when the change involves the buildup of a connective molecular structure which manifests itself over macroscopic portions of the sample. Thus we might expect the dielectric charge polarization arising from the onset at the phase separate interface to be observed first.

The fact that the onset of the phase separation charge polarization is seen at approximately the same time as in the mechanical properties suggests the initial rate of change from a homogeneous system to a heterogeneous two-phase material is rapid and involves initially a large amount of the thermoset precursor generating a morphology which immediately involves large enough particles to be seen by a macroscopic measurement of mechanical properties.

The position of the charge polarization phase separation relaxation peak in ϵ'' can be compared to the predictions of the Maxwell–Wagner–Sillars (MWS) equations, where in Eqs. (5)–(9), the subscript 1 refers to the PPE-rich continuous β-phase and the subsript 2 refers to the α-phase, epoxy-rich occluded particles. Assuming spherical particles whereby $A = 1/3$, with a volume fraction V_2 of the occluded phase equal to the initial thermoset precursor percent and using the values of ϵ_α and σ_α for the neat DGEBA–MCDEA epoxy–amine system at the respective cure temperatures and for ϵ_β and σ_β of the neat PPE; Eq. (8)

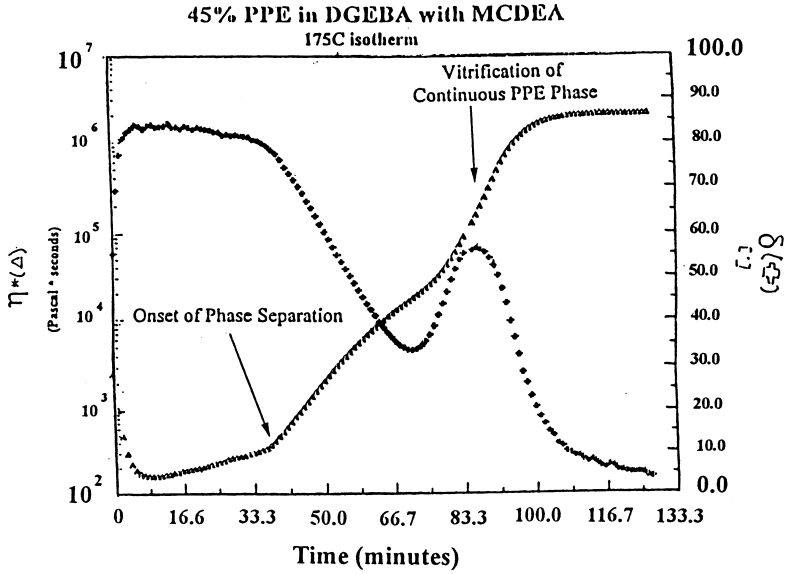

Fig. 3. Dynamic mechanical values of viscosity and loss angle δ for 45% PPE/DGEBA–MEDEA cured at 175°C.

Table 2
Monitoring onset of phase separation time to phase separation (in min). Frequencies: mechanical = 10 rad/s, dielectric = 31 400 rad/s (5 kHz)

Composition of initial homogeneous mixture (wt.% PPE)	Phase separation	Time in min			
		150°C	175°C	200°C	225°C
30%	Mechanical/Dielectric	Heterogeneous from the beginning	15/18	11/15	7/6
45%	Mechanical/Dielectric	54/46	35/36	21/7	12/10
60%	Mechanical/Dielectric	166/130	82/77	43/43	23/24

can be used to calculate, with these assumed values, the MWS relaxation time τ. This relaxation time is related to the respective frequency $f = (2\pi\tau)^{-1}$ where an ϵ'' loss peak should initially occur. These predicted peak values of ϵ'' using the initial volume percents as reported in Table 1 for a 27.3% by volume PPE/epoxy system range from 1.0 to 2.9 kHz over 150 to 250°, for 40.5% PPE from 1.2 kHz at 150°C to 4.1 kHz at 225°C and for 58% PPE from 1.3 kHz at 150°C to 5.2 kHz at 225°C. The observed frequencies for all of the temperatures and the three compositions are in the high kHz frequency range when the ϵ'' peak is first observed as seen for example in Figs. 4 and 5.

The fact that the MWS predicted relaxation times and the observed peaks in $\epsilon''(\omega)$ differ by a factor of ten to several hundred is troubling. Since the exact values of ϵ_β, σ_β, ϵ_α, σ_α and v_α are not known at the onset and during the phase separation process because of the ongoing diffusion and reaction advancement processes described, other MWS predictions of τ_{MWS} were made using different values for the particle shape, and differing values of ϵ_β,σ_β, ϵ_α and σ_α assuming a mixture of PPE and epoxy in each phase. The effect of these "possible values" was at a maximum, a factor of 10 to either increase or decrease τ_{MWS}. Thus use of other possible values of σ and ϵ in the MWS equations could not fully account for the initial high-frequency peaks in $\epsilon''(\omega)$.

Following the onset of phase separation a number of interrelated processes are occurring. First the epoxy–amine *n*-mers are diffusing out of the homogeneous system as the epoxy–amine reaction advances and thereby they becomes less soluble, thus the number and size of these α-phase epoxy-rich particles is changing with time. Similarly the composition of both the α- and the β-phase is changing. As the epoxy–amine reaction advances, the α- epoxy-rich phase becomes more viscous and its conductivity decreases. As the epoxy–amine *n*-mers diffuse out of the PPE-rich β-phase, the β-phase also becomes more viscous as it becomes richer in PPE. Thus the T_g of the continuous PPE-rich phase increases from below the cure temperature both because the T_g of the pure PPE is higher 213°C and because the residual epoxy–amine in the continuous phase is advancing. Insight into these rate processes, is acquired by observing the mechanical and dielectric properties and may provide an explanation for the high frequency peaks in $\epsilon''(\omega)$. A phase diagram schematic of the processes is shown in Fig. 6.

In Table 3 the time of occurrence of the mechanical relaxation peak in δ as shown in Fig. 2 for each of the temperatures and compositions is tabulated. No peak is observed for the 225°C reactions as this temperature is above T_g of the neat PPE. The results show an α-relaxation

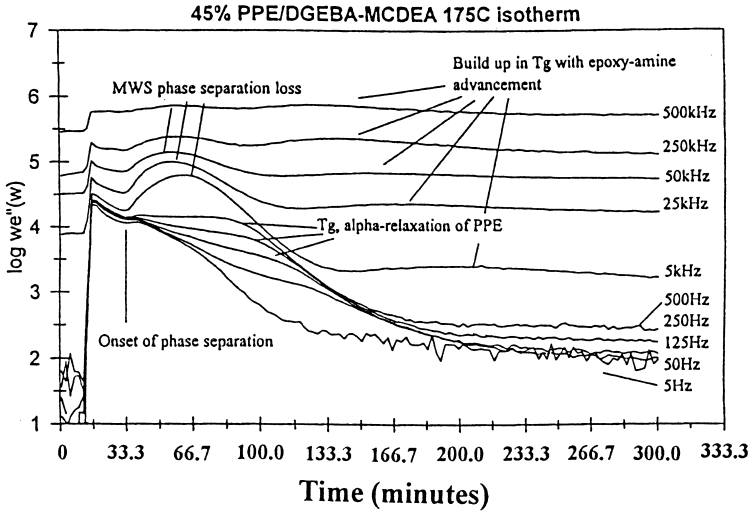

Fig. 4. Frequency dependent values of $\log[\omega\epsilon''(\omega)]$ versus time for 45% PPE/DGEBA–MCDEA at 175°C.

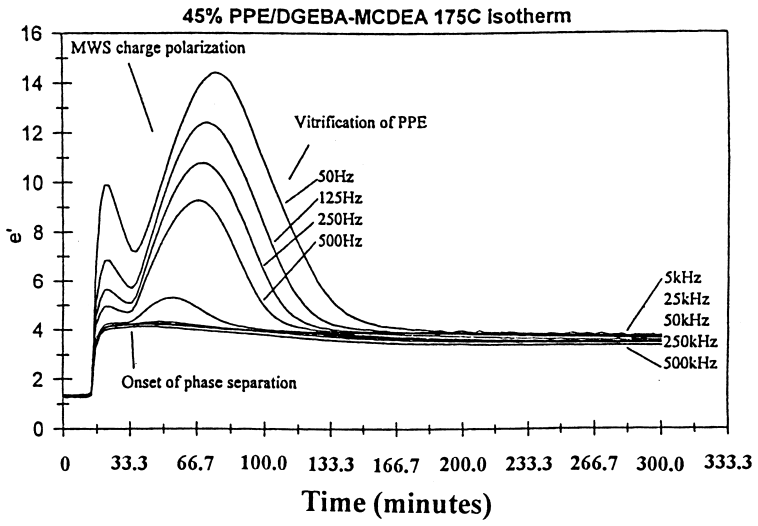

Fig. 5. Frequency dependent values of ϵ' versus time for 45% PPE/DGEBA–MCDEA at 175°C.

peak associated with T_g which occurs at increasingly longer times as the starting homogeneous blend becomes richer in thermoplastic and shorter times as the temperature increases. We can assume the phase separation process is stopped by the vitrification of the PPE-rich phase. At this time the β-phase has become rich enough in PPE such that its T_g is equal to or in the range of the isothermal cure temperature.

The dielectric output is also sensitive to the vitrification of the PPE-rich phase. As indicated in Figs. 4 and 5, the α-relaxation associated with the T_g of the PPE-rich continuous phase can be observed after the magnitude of the charge polarization decreases due to the decrease in σ_α as the epoxy–amine component reacts. The dielectric measurements of the α-relaxation glass transition process are made at high frequencies relative to mechanical measurements and thus they occur at shorter times. The 500 Hz dielectric measured times of occurrence of the

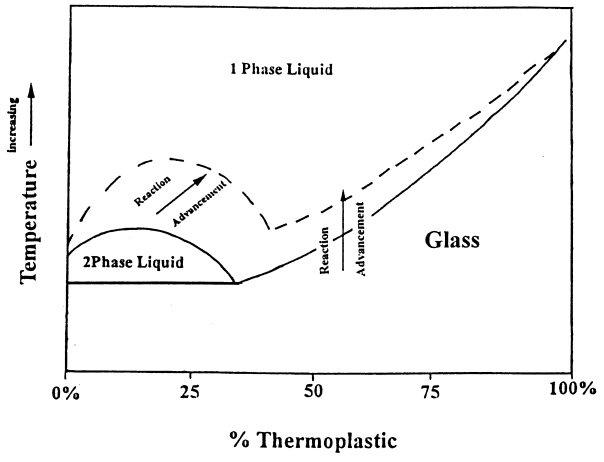

Fig. 6. Schematic of the changing phase diagram of the PPE/DGEBA–MCDEA mixture as the epoxy–amine reaction advances forming less soluble *n*-mers.

α-relaxation T_g relaxation for the three systems and three temperatures examined are reported in Table 3.

The dielectric relaxation peaks associated with the T_g fo the β- PPE-rich phase in Fig. 4 are identified in the 5 kHz–125 Hz range. The α-relaxation process in polymer systems can be observed at higher frequencies, e.g. 5 –500 kHz, but these peaks are masked by the much larger charge polarization increase in the value of ϵ^*. Nevertheless, it is certainly likely that lack of agreement between the measured τ and the predicted τ_{MWS} is at least partically a result of the peak in $\epsilon''(\omega)$ during the onset of phase separation arising from a combination of a τ_{MWS} interfacial relaxation process and the high frequency onset of the α-relaxation vitrification process of the PPE-rich phase.

Next, the net time involved in the phase separation processes as monitored by the elapsed time to mechanical vitrification of the PPE-rich phase minus the onset of phase separation is examined. These times are reported in Table 4. The time decreases as the temperature increases indicating the kinetics of the epoxy–amine reaction are occurring faster as well as the diffusion rate of the phase separation process in a less viscous media. Thus the higher isothermal temperature has a greater effect on the kinetics of the newly forming *n*-mers and their diffusion into the α-phase then the increase in purity of the PPE-rich phase required to reach the higher T_g associated with the higher cure temperature. Second the smaller difference in time at each temperature for 30% PPE, relative to 45% PPE and 60% PPE again suggests the kinetics of this reaction are initially very rapid in the higher concentration, lower viscosity 30% PPE, 70% epoxy–amine system such that this system is almost able to catch up to and attains a pure enough PPE-rich continuous phase to vitrify before the initially much richer 60%, PPE, highly viscous, system.

Table 5 reports values of the α-relaxation T_g peak for the occluded epoxy-rich α-phase as observed by the dielectric measurements. Also reported in Table 5 are the values for

Table 3
Monitoring buildup in T_g of continuous PPE phase as epoxy diffuses out time to vitrification of PPE phase (min). Frequencies: mechanical = 10 rad/s, dielectric = 3141 rad/s (500 Hz)

Composition of initial homogeneous mixture (wt.% PPE)	PPE phase vitrification	Time in min to PPE continuous phase vitrification		
		150°C	175°C	200°C
30%	Mechanical/Dielectric	0/65	63/26	47/19
45%	Mechanical/Dielectric	153/108	86/60	59/29
60%	Mechanical/Dielectric	243/233	132/115	90/65

the neat DGEBA–MCDEA system under similar isothermal temperatures. From Table 5 it is quickly apparent that the epoxy–amine-rich 30% PPE system has elapsed times for the dielectric vitrification peak of the α-phase which are close to those for the neat epoxy, indicating this dielectric loss peak is due to the vitrification of the epoxy–amine. The fact that the dielectric measurements are sensitive to the vitrification of the occluded epoxy–amine-rich phase in an already vitrified continuous matrix is undoubtedly due to the fact that the epoxy is highly polar, particularly relative to the PPE. Initially it was thought that the mechanical measurements would be most sensitive to the vitrification of the continuous phase. Little if any sensitivity to vitrification of the occluded phase, particularly when the continuous phase vitrifies first was expected. But when torsion specimens were cast and advanced, it was possible to detect a vitrification peak of the epoxy-rich occluded phase in both the 30% PPE and the 60% PPE mixtures. However this measurement process is much more time consuming and less accurate than the dielectric measurements do to the need to advance the reaction, quench and restart in the rheometer.

In Table 6 the elapsed time from the onset of phase separation to vitrification of the occluded epoxy–amine rich α-phase is reported. If these values were similar to the neat epoxy–amine values in Table 4 at the same temperature and frequency, one could assume the epoxy–amine reaction rate is significantly decreased up to the time of phase separation due to dilution effects in the homogenous PPE epoxy–amine mixture. After phase separation the epoxy–amine goes into a high concentration as the occluded phase. For the 30% PPE, the richest system in epoxy–amine, the results in Table 6 show a shorter time to vitrification from the onset of phase separation compared to the neat epoxy. In Table 4 the absolute total times to vitrification are similar. This suggests the epoxy–amine is advancing prior to phase separation at probably a reduced rate due to dilution and that vitrification is achieved at a lower level of conversion than in the neat epoxy–amine because some of the high T_g PPE thermoplastic remains in the occluded phase.

On the other hand in the 60% PPE, system with the lowest concentration of epoxy–amine, the elapsed time to vitrification after phase separation is slightly longer than the vitrification for the neat system. This suggests that as the system becomes richer in PPE, because of the decrease in concentration of the epoxy–amine in the homogeneous system, a dilution effect, the reaction rate is decreased significantly. The relatively close agreement of the elapsed time to vitrification after phase separation with the neat system also supports the view that the major portion of the epoxy–amine in the starting mixture phase separates immediately with the onset of the phase separation process at which time the epoxy–amine reacts in the more highly concentrated α-phase.

Table 5
Monitoring reaction advancement, build up in T_g of epoxy-rich occluded phase from α-relaxation peaks. Elapsed time in min to dielectric α-relaxation peak in ϵ''

Composition of initial homogeneous mixture (wt.% PPE)	Frequency (kHz)	Elapsed time (min)		
		150°C	175°C	200°C
0%	5	228	140	126
30%	5	231	144	127
45%	5	255	199	143
60%	5	392	N/A	230
0%	50	197	121	69
30%	50	189	108	83
45%	50	224	141	99
60%	50	345	216	141
0%	500	167	99	45
30%	500	150	84	67
45%	500	177	112	73
60%	500	291	167	104

Table 4
Time to mechanical vitrification of PPE phase minus (Dielectric/Mechanical) phase separation (min). Frequencies: mechanical = 10 rad/s, Dielectric = 3141 rad/s (500 Hz)

Composition of initial homogeneous mixture (wet. % PPE)	PPE phase vitrification	Time to mechanical vitrification minus time of dielectric or mechanical phase separation		
		150°C	175°C	200°C
30%	Minus Dielectric/Minus Mechanical	–	45/48	37/36
45%	Minus Dielectric/Minus Mechanical	107/99	50/51	40/38
60%	Minus Dielectric/Minus Mechanical	113/77	55/50	46/47

Table 6
(Dielectric α-relaxation peak time) − (Dielectric phase separation time). Elapsed time in min to α-relaxation based on peak in ϵ''

Composition of initial homogeneous mixture (wt.% PPE)	Frequency (kHz)	Elapsed time (min)			
		150°C	175°C	200°C	225°C
0%	5	228	140	126	N/A
30%	5	N/A	126	112	N/A
45%	5	209	163	136	N/A
60%	5	262	N/A	187	N/A
0%	50	197	221	69	N/A
30%	50	N/A	90	68	N/A
45%	50	178	105	92	N/A
60%	50	215	139	98	N/A
0%	500	167	99	45	N/A
30%	500	N/A	66	52	N/A
45%	500	131	76	66	N/A
60%	500	*161	90	61	N/A

Finally, it is important to report that as already shown in Table 1, the final volume percentages in the PPE-rich continuous phase are close to but slightly larger than the initial volume percentage of PPE. The variation is higher in the 60% PPE mixture. This supports the conclusions already discussed that the epoxy–amine rapidly diffuses out as the occluded phase in the lower viscosity 30% PPE mixture and that this process is slowed down due to dilution and viscosity in the lower epoxy concentration more viscous 60% PPE mixture, so much so that residual epoxy is apparently trapped in the continuous phase.

Table 1 also supports earlier results, that the final morphology as evidenced by the size of the occluded particles is strongly influenced by these kinetic dilution effects, diffusion, and viscosity conditions during phase separation.

5. Conclusions

Both mechanical and dielectric measurements are good techniques to monitor the onset of phase separation and reaction advancement which produces a buildup in T_g in both the continuous and occluded phases in thermoplastic–thermoset reactive processing systems. In the case of the PPE/DGEBA–MCDEA system, the phase separation process initially occurs rapidly involving a large amount of the epoxy–amine diffusing into the occluded phase. The rate of the epoxy–amine reaction in the epoxy-rich 30% PPE mixture is approximately equal to that in the neat epoxy–amine system due to two opposing effects, a slower reaction rate due to dilution and viscosity and a lower level of conversion at vitrification due to the presence of high T_g PPE. In the 60% PPE mixture, the dilution effect of the PPE has a large affect on decreasing the reaction rate and achievement of vitrification in each phase. Both the dielectric and mechanical measurements detect the buildup in T_g of the PPE-rich continuous phase following the onset of phase separation as the epoxy–amine *n*-mers diffuse out. The dielectric measurements are also sensitive to vitrification of the highly polar occluded epoxy–amine phase. For all three PPE epoxy–amine systems, the continuous thermoplastic-rich phase vitrifies first, followed by vitrification of the thermoset as occluded particles. Finally, the results show as evidenced by the size of the occluded particles and the composition of the continuous phase that the morphology is strongly influenced by the kinetics, diffusion, and viscosity conditions during phase separation.

Acknowledgements

Support from CNRS in France, the NSF Foundation INT 9726207 and NSF Center of Excellence at VPI MR 912004.

References

[1] Williams R, Rozenberg B, Pascault JP. Adv Poly Sci 1997;128:95.
[2] Rubber-modified thermoset resins. In: Riew CK, Gillham JK, editors. Adv Chem Ser 208, Washington, DC: Am Chem Soc, 1984.
[3] Rubber toughened plastics. In: Riew CK, editor. Rubber toughened plastics. Adv Chem Ser 222. Washington, DC: Am. Chem. Soc, 1989.
[4] Riew CK, Kinloch AJ. Toughened plastics 1: science and engineering. In: Riew CK, Kinloch AJ, editors. Adv Chem Ser 223, Washington, DC: Am Chem Soc, 1993.
[5] Sperling LH, Heck CS, An JH. In: Utracki LA, Weiss RA, editors. Multiphase polymers: blends and ionomers. Adv Chem Ser 395. Washington, DC: Am Chem Soc, 1989.
[6] Eklind H, Mauer F, Stechman P. Polymer 1997;38(5):1047.
[7] Venderbosch R, Meijer H, Lemstra P. Polymer 1994;35(4):4349.
[8] Poncet S. CNAM Report: Transformation of PPE with the aid of a reactive solvent and an extruder C.N.A.M. Lyon, 1996.
[9] Mackinnon AJ, Jenkins AD, McGrail PT, Petrick RA. Macromolecules 1992;25:3492.
[10] Raghava RS. J Polym Sci—Polym Phys 1987;25:1017.
[11] Murakami A, Sanders D, Ooishi K, Yoshiki T, Saito M, Wantanabe O, Takezawa M. J Adh 1992;39:227.
[12] Kinloch AJ, Yuen ML, Jenkins SD. J Mat Sci 1994;29:3781.
[13] Girard-Reydet E, Vicard V, Pascault J P, Sautereau H. J Appl Polym Sci 1997;65:2433.
[14] Girard-Reydet E, Riccardi CC, Sautereau H, Pascault JP. Macromolecules 1995;28:7599.
[15] Eloundou JP, Fève M, Gerard JF, Harran D, Pascault JP. Macromolecules 1996;29:6907.
[16] Kranbuehl D. In: Runt J, editor. Dielectric spectroscopy of polymeric mats, 303. Washington, DC: Am Chem Soc, 1997.
[17] Alig I, Jenninger W. J Polym Sci B Polym Phys 1998;36:2461–2470.
[18] Mijovic J, Winnie Tee CF. Macromolecules 1994;27:7287–7293.
[19] Parthum MB, Johari G. Macromolecules 1992;25:3254–3263.
[20] Mathieu C, Boiteux G, Seytre G, Villain R, Dublineau P. J Non-Cryst Solids 1994;172:1012–1016.
[21] Deng Y, Martin G. Macromolecules 1994;27:5141–5146.
[22] Companik J, Bidstrup S. Polymer 1994;35:4823–4840.
[23] Kranbuehl DE. J Non-Cryst Solids 1991;130:930–936.
[24] Brown JM, Srinivasan S, Ward T, Loos AC, Hood D, Kranbuehl D. Polymer 1996;37:1691–1696.
[25] MacKinnon AJ, Jenkins SD, MacGrail PT, Pethrick RA. Polymer 1993;34:3252–3263.
[26] MacKinnon AJ, Jenkins SD, MacGrail PT, Pethrick RA. Macromolecules 1992;25:3492–3499.

[27] Delides CG, Hayward D, Pethrick A, Vatalis AS. Europ Polym J 1992;28:505–512.
[28] Maistros G, Block H, Bucknall CB, Partridge IK. Polymer 1992;33:4470–4478.
[29] Korkakas G, Gomez CM, Bucknall CB. Plastic Rubbers Composites Process Appl 1993;19:285.
[30] Kranbuehl D, Kim T, Liptak SC, McGrath JE. Polym Prepr 1993;34:488–489.
[31] Vinh-Tung C, Boiteux G, Seytre G, Lachewal G, Chabert B. Polym Comp 1996;17:767.
[32] Friedrich K, Vinh-Tung G, Boiteux G, Peytre G, Ulanski J. J Appl Polym Sci 1997;65:2529–2543.
[33] Lestriez B, Maazouz A, Gerard JF, Sautereau H, Boiteux G, Seytre G, Kranbuehl D. Polymers 1998;39(26):6733–6742.
[34] Sillars RW. J Inst Electr Engng 1937;80:378.
[35] Van Beek LHK. Dielectric behavior of heterogeneous systems. Progr Dielectrics 1967;7:69–114.
[36] Bánhegyi G. Colloid Polym Sci 1986;264:1030–1050.